



THE UNIVERSITY *of* EDINBURGH

Edinburgh Research Explorer

A portable high-pressure stress cell based on the V7 Paris-Edinburgh apparatus

Citation for published version:

Bromiley, G, Redfern, SAT, Le Godec, Y, Hamel, G & Klotz, S 2009, 'A portable high-pressure stress cell based on the V7 Paris-Edinburgh apparatus' High Pressure Research, vol. 29, no. 2, pp. 306-316. DOI: 10.1080/08957950902747411

Digital Object Identifier (DOI):

[10.1080/08957950902747411](https://doi.org/10.1080/08957950902747411)

Link:

[Link to publication record in Edinburgh Research Explorer](#)

Document Version:

Peer reviewed version

Published In:

High Pressure Research

Publisher Rights Statement:

This is an Author's Accepted Manuscript of an article published in High Pressure Research 29(2): 306-316 copyright Taylor & Francis (2009) available online at: <http://www.tandfonline.com/> (10.1080/08957950902747411)

General rights

Copyright for the publications made accessible via the Edinburgh Research Explorer is retained by the author(s) and / or other copyright owners and it is a condition of accessing these publications that users recognise and abide by the legal requirements associated with these rights.

Take down policy

The University of Edinburgh has made every reasonable effort to ensure that Edinburgh Research Explorer content complies with UK legislation. If you believe that the public display of this file breaches copyright please contact openaccess@ed.ac.uk providing details, and we will remove access to the work immediately and investigate your claim.



Author's final 'post-print' version. The final article was published in High Pressure Research copyright Taylor & Francis (2009).

Cite As: Bromiley, G, Redfern, SAT, Le Godec, Y, Hamel, G & Klotz, S 2009, 'A portable high-pressure stress cell based on the V7 Paris-Edinburgh apparatus' *High Pressure Research*, vol 29, no. 2, pp. 306-316.

DOI: 10.1080/08957950902747411

A portable high-pressure stress cell based on the V7 Paris-Edinburgh apparatus

Geoffrey D. Bromiley^{a,b*}, Simon A.T. Redfern^a, Yann Le Godec^c, Gérard Hamel^c and Stefan Klotz^c

^a*Department of Earth Sciences, University of Cambridge, Downing Street, Cambridge, CB2 3EQ, UK;*

^b*present address: School of GeoSciences, University of Edinburgh, Grant Institute, The King's buildings, West Main Road, Edinburgh, EH9 3JW, UK*

^c*IMPC, Université P&M Curie, 140 Rue Lourmel, F-75015, France.*

We describe a new device, based on a V7 Paris-Edinburgh press, for torsional testing of material at pressures up to 7 GPa (extendable to 15 GPa). Samples are deformed using a simple shear geometry between opposed anvils by rotating the lower anvil, via a rotational actuator, with respect to an upper, stationary, anvil. Use of conical anvil profiles greatly increases sample dimensions compared to other high-pressure torsional apparatus. Samples of polycrystalline Zr (2mm thick, 3.5 mm diameter) have been sheared at strains exceeding $\gamma \sim 1.5$ at constant strain rate at pressures from 1.8 to 5 GPa, and textural development studied by electron microscopy. Use of amorphous-boron-epoxy gaskets means that nearly simple shear of samples can be routinely achieved. This apparatus allows study of the plastic and anelastic behaviour of materials under high-pressure, and is particularly suited for performing *in-situ* investigations using synchrotron or neutron radiation.

Keywords: High pressure; deformation; torsion; anelastic

Corresponding author. Email: geoffrey.bromiley@ed.ac.uk

1. Introduction

The Paris-Edinburgh apparatus is an opposed anvil device in which a sample, encased in a deformable gasket, is pressurised between opposed anvils made of tungsten carbide, sintered diamond, or cubic boron nitride, providing sample volumes up to 100 mm³. In opposed anvil devices such as this, it is theoretically possible to deform samples at simultaneous high-pressure by rotating one of the anvils with respect to the opposite anvil, thereby imparting a torque on the sample and sample assembly [1]. Such a geometry was originally described in the 1930s, although application of such devices has remained limited (e.g. [2, 3]). Recently, Yamazaki and Karato [4] described a similarly modified Drickamer-type opposed anvil apparatus for deforming samples at pressures up to at least 15 GPa. The key advantages that devices such as these have are that: (a) the apparatus can be designed to be small and relatively portable, allowing it to be transported to synchrotron sources and not tied to any one location, (b) very high stresses can be imparted on samples at controlled strain rates, and (c) pressurisation and deformation of samples are, by nature of sample geometry, decoupled, although in practise this is challenging to implement. Here, we describe a new design for an opposed anvil deformation cell which develops some of the concepts introduced by Yamazaki and Karato [4]. It is based around the Paris-Edinburgh loading frame, which is a mature and widely adopted platform used for high-pressure, and recently simultaneous high-pressure/high-temperature studies, and has been optimised for use at central facilities (synchrotron and neutron sources), both in terms of overall size and weight of the press frame (enhancing portability) and anvil and sample assembly design (maximising sample volume).

2. Description of experimental technique

2.1 High-pressure apparatus

Our high-pressure loading frame is based on a modified V7 (450 tonne) Paris-Edinburgh apparatus (see Le Godec et al. [5] for general description). The only significant modification to the loading frame is a 50% elongation of the four tie rods; this provides the additional space between the platens required to accommodate additional rotation components. A similar elongation of tie-rods for a V4 Paris-Edinburgh cell was previously described by Dobson et al. [6]. A schematic cross section of the apparatus is shown in Figure 1, and an annotated photograph in Figure 2. The press frame is inverted relative to normal use, so that the breech (H) is located on the underside of the apparatus. This has advantages for loading and unloading sample assemblies. By unscrewing the breech, the entire rotation and thrust assembly (parts C to N) are lowered, increasing the gap between the anvils (O) and (N) by several centimetres. Samples can simply be loaded and unloaded without having to remove any additional components, resulting in sample exchange rates of a few minutes. Load is applied to the anvils via a hydraulic ram (A) located in the upper plate. Load acts on the upper anvil (O) via a system of anvil seats and spacers. Load on the lower anvil is also imparted through the press frame via the thrust bearings (I), conical spacer (J), central hardened steel piston (D) and lower anvil seat. The central piston (D) passes through a hole in the centre of the reduction gearing (M), thereby ensuring that no load is placed on the fragile gearing unit. Torque is applied to the sample by rotating the lower anvil whilst ensuring that the upper anvil remains stationary, using an externally mounted servo, timing belt and high-ratio reduction gearing (as described by Yamazaki and Karato [4]). The external DC servo (G) (Harmonic Drive©, PMA-8A-100-01-E1000ML) is linked to an encoder and contains a 100:1 reduction gear on the servo head. The servo is linked to a 161:1 ratio hollow-shaft reduction

gearing unit (M) (Harmonic Drive© HFUS-32-160-2UH) (max output torque 314 Nm) via a steel reinforced 3:1 timing belt (E), resulting in a total gear ratio of 48300:1. The output from the reduction gearing is connected to the lower (rotating) anvil via the anvil housing. The hardened steel supports for the lower anvil and anvil seats are hexagonal and sit in a hexagonal space inside the housing unit (Figure 3) to ensure that torque from the gearing is transferred to the anvil. Carbide inserts in both anvils are shaped to prevent rotation of the inserts within the housing (steel supports N and O), and have a circular outer geometry on the sample side and an oval geometry on the seat side (Figures 3 and 4). The upper (stationary) anvil is identical to the lower (rotating) anvil. In this case, the hexagonal shape of the anvil housing fits inside an insert in an additional plate (B in Figures 1-3) that in turn, is fastened to two of the tie rods. This plate prevents rotation of the upper anvil, ensuring that torque is only accommodated through deformation of the sample assembly.

2.2 Anvil and sample assembly

The geometry of the inner face of the carbide anvils is identical to that described in Le Godec et al. [7], and which is now standard in high-P/high-T Paris-Edinburgh cell experiments. This anvil profile is described as ‘conical’ and differs from the standard toroidal anvil design used in many high-pressure applications in that the inner anvil faces are flat and perpendicular to the axis of sample compression. This anvil geometry has many intrinsic advantages, most notably good mechanical strength and reduction in uniaxial stress (which is of prime importance in minimising additional sources of sample deformation) and large comparative sample volume. Furthermore, sample pressure using conical anvil profiles has been well characterised in recent years in several series of on-line (synchrotron) and off-line tests.

Samples were loaded into a hole in the centre of fired pyrophyllite or amorphous boron-epoxy (a-B epoxy) gaskets which had a shape mirroring the profile of the opposing

anvils (Figure 4). Pyrophyllite gaskets were machined from commercial grade material that had been heat treated [7, 8]. a-B-epoxy gaskets were produced using a novel hot-pressing technique. A 4:1 ratio (by weight) of amorphous boron and epoxy resin was mixed in an agate mortar. This mixture was then modelled into small cylinders and polymerised at 100 °C for 45 minutes to harden. Cylinders were then compacted up to 15 kbars over a 5 minute period in a standard piston-cylinder press. The resulting boron-epoxy cylinders are very hard and have very low porosity, and were machined using tungsten carbide tools into the final gasket shape. Machinable polycrystalline MgO spacers (fired in air at 1600°C for 5 hours) were used to locate the sample in the centre of the assembly. For experiments described here, we used anvils with a 10 mm truncation and gaskets of 10 mm outer diameter and with an internal sample volume diameter of 3.5 mm (Figure 4). Sample thickness in this assembly is 2.0 mm. In order to prevent excessive gasket flow during pressurisation and deformation, teflon containment rings were fitted around the outside of the gaskets in all runs, as used in the high-P/high-T assemblies of Le Godec [7].

2.3 Pressure calibration

The pyrophyllite and a-B epoxy gaskets used in the roPEC have previously been well calibrated in a series of *in-situ* X-ray diffraction experiments, using internal NaCl and MgO pressure calibrants, as shown in Figure 5. Additional experiments were performed using the roPEC apparatus to verify these known pressure calibrations using the I-II phase transition in bismuth (as determined by the marked drop in electrical resistivity that accompanies this transition [9]). The oil pressure at which this transition occurred corresponded, within error, to existing sample pressure calibrations shown in Figure 5 for both pyrophyllite and a-B epoxy gaskets. At slightly higher pressure, bismuth is expected to undergo a further transition (BII-

III), accompanied by a much smaller change in resistivity, although this was not observed in the pressure calibration experiments performed using the roPEC apparatus.

3. Deformation of Zr

We performed a series of experiments in which we deformed polycrystalline Zr at varying pressures to test the apparatus. Zr has a hexagonal-centred-cubic (hcp) structure at room temperature and ambient pressure. At 2.2 GPa, room T, Zr undergoes a phase transition to a hexagonal structure called the ω phase [10]. The ω phase is not close-packed (space group number 191, $P6/mmm$), and once formed is metastable at ambient pressure [11]. The starting material was high-purity, annealed, polycrystalline Zr rod and was purchased pre-annealed. SEM investigation revealed that it had a well-equilibrated, fine-grained texture consisting of 5-10 μm equiaxial grains, and no further preparation prior to deformation studies was deemed necessary. The material was lathed to 3.5 mm diameter from which 2 mm discs were cut using a wire saw with silicon carbide flux. Surfaces of these discs were lightly polished using Si-C paper and diamond suspensions (down to 5 μm). These discs were then cut in half lengthwise using a wire saw and Si-C paste and cleaned in high-purity acetone in an ultrasonic bath for 30 minutes. A thin sheet of gold foil was inserted between the two halves prior to loading in the sample assembly. This foil was used as an internal strain marker of the type described by Yamasaki and Karato [4] (see their Figure 6). In all deformation experiments, samples were loaded into an assembly as shown in Figure 4, using either pyrophyllite or a-B epoxy gaskets.

Deformation experiments were performed at pressures ranging from 1.8 to 5.0 GPa. Upon loading, samples were pressurised at a rate of 10 bars (oil pressure)/minute to the desired value. Pressure was maintained at this value for a further 10-30 minutes to allow sample and gasket equilibration. The servo was then rotated at a fixed rate of 50 rpm (on the

servo head), corresponding to a sample rotation rate of 1.035×10^{-3} rpm or approximately 22.3°/hour, again whilst continuously maintaining sample pressure. Servo output velocity, position and current were continually monitored and velocity controlled via a PC connected to the servo encoder. This information was used to monitor the rate of sample deformation. Actual rotation rate of the lower anvil with respect to the upper anvil could easily be verified by visual observation. Output current from the servo gives a first approximation of the torque applied to the sample assembly by the reduction gearing, although it is expected that some loss of torque will occur during transfer to the sample from the external servo and that most torque is used to deform the gasket material. At all pressures, only minor variation in servo output velocity (less than 1%) was observed once the gasket/sample had reached steady-state equilibrium during deformation. During pressurisation and deformation, movement of the ram was monitored and recorded using a needle gauge.

In all runs, considerable changes in sample microstructure as a result of sample deformation were observed (Figures 6). After deformation, grains in all samples were elongated in the direction of sample shear and showed evidence of considerable plastic deformation. As noted by Yamasaki and Karato [4], a possible problem with opposed anvil, rotational deformation devices is that considerable sample deformation may occur during initial sample pressurisation. Yamasaki and Karato [4] attempted to minimise sample compression during pressurisation by surrounding samples with a softer, deformable material to prevent excessive sample flow, as well as reducing sample thickness to 0.4 mm. In the present study, we find that the use of conical anvil profiles (as opposed to the flat-faced anvil head profiles used in Drickamer apparatus) greatly reduces initial sample compression (i.e. plastic deformation) during pressurisation. Figure 7 shows a plot of sample thickness during experimental runs under various compositions (comparable to Figure 7 of Yamasaki and Karato [4]). In all experiments, some initial sample compression occurred during

pressurisation. However, sample compression is noticeably reduced when a-B epoxy gaskets are used, presumably due to reduced gasket flow compared to pyrophyllite (consistent with differences in pressure calibration, as shown in Figure 5). Additional sample compression occurs during deformation, although once again, differences between gasket performance indicate that this is largely related to the degree of additional gasket flow during shear. Use of a-B epoxy gaskets results in an acceptable level of sample compression during pressurisation (approximately 5-10% change in sample thickness at pressures up to 5 GPa), implying that samples are deformed under almost pure simple shear, with an insignificant component due to initial uniaxial compression. Gasket flow during initial pressurisation and during prolonged deformation is also evident from data on ram movement (Figure 8). Once run pressure is attained, prior to deformation, gasket flow quickly tails off, and the sample assembly rapidly attains an equilibrium response due to compression. Once the lower anvil is rotated and the assembly sheared, there is a progressive (much smaller) flow response of the assembly, evident in continual ram movement needed to maintain run pressure.

Change in the geometry of the Au foil strain marker was measured after experimental charges were recovered. Figure 9 shows a typical recovered sample. For small degrees of rotation ($<90^\circ$), the sample could be removed from the assembly in two pieces, with the Au foil adhering to one piece (as shown). For higher degrees of rotation (and at higher run pressures), samples were recovered as one piece. In all runs, angle of rotation was, within error, the same as that calculated from the servo head position, implying that torque from the apparatus was effectively transferred to the sample, with minimal slipping of sample assemblies or components of the assemblies, with respect to the anvils.

Output current from the servo motor can be used as an approximate indication of torque applied to the sample assembly. Figure 10 shows a plot of current vs angle of rotation for several experiments. Current/torque increases rapidly up to approximately 5° rotation,

after which it levels off. In all runs performed under load, there was an additional, slight increase in current/torque during prolonged sample deformation. There is a clear relationship between sample pressure (load) and torque, with much greater torque needed to deform sample assemblies held under greater loads. Both these observations were also made by Yamasaki and Karato [4] in relation to their rotational Drickamer apparatus. Significant differences between pyrophyllite and a-B epoxy gasket materials are also noted. Although a-B epoxy gasket flow during deformation is greatly reduced in comparison to pyrophyllite gaskets, torque required to deform a-B epoxy gaskets is significantly lower at the same given pressure (even when account for greater load required to attain similar sample pressures using less efficient pyrophyllite gaskets). Differences between applied torque required for different gasket materials highlight that most torque applied by the gearing system is probably used to deform parts of the sample assembly other than the sample itself.

4. Future development of the roPEC apparatus

Anvil and gasket geometry used in the roPEC is the same as that used in the high-pressure/temperature Paris-Edinburgh cell described by Le Godec et al. [7]. In this assembly, high sample temperatures are achieved by passing an electrical current through an internal resistance furnace, typically made from graphite. This assembly could, with minor modification, be used in the roPEC to permit deformation studies at simultaneous high-pressures and temperatures.

The maximum sample pressure achievable in a Paris-Edinburgh type apparatus is limited by the mechanical strength of the anvils. For the roPEC, experiments have been successfully performed up to 5 GPa, although the same anvil/gasket geometry has been used in a V4 press to achieve sample pressures (determined by internal pressure calibrants) of up to 8 GPa. Higher sample pressures could be achieved by using smaller anvil/gasket sizes. The

current anvil face used in the roPEC is 3.5 mm diameter, with a gasket width of 10 mm (3.5/10 assembly) as shown in Figure 4. Experience from high-temperature Paris-Edinburgh cell experiments suggests that use of 7/2 and 5/1.5 anvil/gasket assemblies should permit attainment of sample pressures up to 10 and 15 GPa, respectively [12]. This is somewhat lower than the maximum pressure that can be achieved using a Drickamer-type opposed anvil device, although this is more than offset by the significant increase in sample volume that is achievable using shaped anvil faces and the reduction in sample stress during initial compression.

The Paris-Edinburgh apparatus has been designed chiefly for performing *in-situ* investigations using neutron and synchrotron radiation at high pressure, and more recently, simultaneous high-pressure/temperature. Small size and weight of the loading frame also means that Paris-Edinburgh cell apparatus is portable. This has the inherent advantage that apparatus does not have to be constructed on dedicated beamlines. The total weight of our modified roPEC is less than 150 kg, meaning that the device, whilst heavier than a normal V7 press, is still not tied to any one location, and fits well within the equipment weight and size limits of general synchrotron beamlines. The roPEC apparatus has also been constructed so that access to the sample is maximised and only constrained by the four tie rods (i.e. implying that diffraction data could be obtained from a sample over a wide scattering angle). Use of this apparatus at a synchrotron facility will mean that sample stress and strain rate can be determined from X-ray measurements and X-ray tomographic imaging. To verify the suitability of the sample assembly materials for employment of *in-situ* tomographic imaging, we have conducted initial measurements of recovered samples using a commercial lab-based X-ray tomographic machine. As can be seen in Figure 11, transparency of the sample assembly is excellent, and the geometry of the strain marker can clearly be determined, even though the gasket material used for testing was fired pyrophyllite. Use of a-Boron gaskets

would further enhance transparency of the gasket considerably. The roPEC apparatus has been designed and tested for use with tungsten carbide anvils. However, for *in-situ* experiments using X-ray radiation, other anvil materials might be preferred. For example, X-ray transparent sintered diamond or cubic BN anvils would increase the volume of the cell assembly that could be ‘seen’ in tomographic images, and for measuring strain, would make it easier to observe a greater proportion of sample Debye rings.

Acknowledgements

The authors would like to thank Colin Morrison and Paul Taylor (Dept. Earth Sciences, University of Cambridge), and John Adams (Harmonic Drive UK Ltd) for help in the design and construction of the roPEC. They also thank Shun-ichiro Karato for helpful discussions regarding the rotational Drickamer apparatus and an informative visit to Yale during the design stage for the roPEC. This project was supported by NERC grant LBZF/039 (to SAT Redfern and MT Dove).

References

- [1] J. Bridgeman, *Studies in large plastic flow and fracture*, McGraw-Hill, New York, 1952.
- [2] A. Concustell, J. Sort, S. Surinach, A. Gebert, J. Eckert, A.P. Zhilyaev, M.D. Baro, *Severe plastic deformation of a Ti-based nanocomposite alloy studied by nanoindentation*, *Intermetallics* 15 (2007), pp. 1038-1045.
- [3] R. Valiev, R.K. Islamgaliev, I.V. Alexandrov, *Bulk nanostructured materials from severe plastic deformation*, *Prog. Mat. Sci.* 45 (2000), pp. 103-189.
- [4] Y. Yamasaki, and S. Karato, *High-pressure rotational deformation apparatus to 15 GPa*, *Rev. Sci. Instr.* 72 (2001), pp. 4207-4211.
- [5] Y. Le Godec, G. Hamel, D. Martinez-Garcia, T. Hammouda, V.L. Solozhenko, S. Klotz, *Compact multianvil device for in situ studies at high pressures and temperatures*, *High Press. Res.* 25 (2005), pp. 243-253.
- [6] D. Dobson, J. Mecklenburgh, D. Alfe, I.G. Wood, M.R. Daymond, *A new belt-type apparatus for neutron-based rheological measurements at gigapascal pressures*, *High Press. Res.* 25 (2005), pp. 107-118.
- [7] Y. Le Godec, M.T. Dove, S.A.T. Redfern, M.G. Tucker, W.G. Marshall, G. Syfosse, S. Klotz, *Recent developments using the Paris-Edinburgh cell for neutron diffraction at high pressure and high temperature and some applications*, *High Press Res.* 23 (2003), pp. 281-287.
- [8] Y. Le Godec, M.T. Dove, D.J. Francis, S.C. Kohn, W.G. Marshall, A.R. Pawley, G.D. Price, S.A.T. Redfern, N. Rhones, N.L. Ross, P.F. Schofield, E. Schooneveld, G. Syfosse, M.G. Tucker, M.D. Welch, *Neutron diffraction at simultaneous high temperatures and pressures, with measurement of temperature by neutron radiography*, *Min. Mag.* 65 (2001), pp. 737-748.

- [9] F. Bundy, *Phase diagram of bismuth to 130 000 km/cm², 500°C*, Phys. Rev. 110 (1958), pp. 314-318.
- [10] X. Hui, S.J. Duclos, A.L. Ruoff, Y.K. Vohra, *New high-pressure phase-transition in zirconium metal*, Phys. Rev. Lett. 64 (1990), pp. 204-207.
- [11] S. Sikka, Y.K. Vohra, R. Chidambaram, *Omega phase in materials*, Prog. Mat. Sci. 27 (1982), pp. 245-310.
- [12] G. Morard, M. Mezouar, N. Rey, R. Poloni, A. Merlen, S. Le Floch, P. Toulemonde, S. Pascarelli, A. Sam-Miguel, C. Sanloup, G. Fiquet, *Optimization of Paris-Edinburgh press cell assemblies for in situ monochromatic X-ray diffraction and X-ray absorption*, High Press. Res. 27 (2007), pp. 223-233.

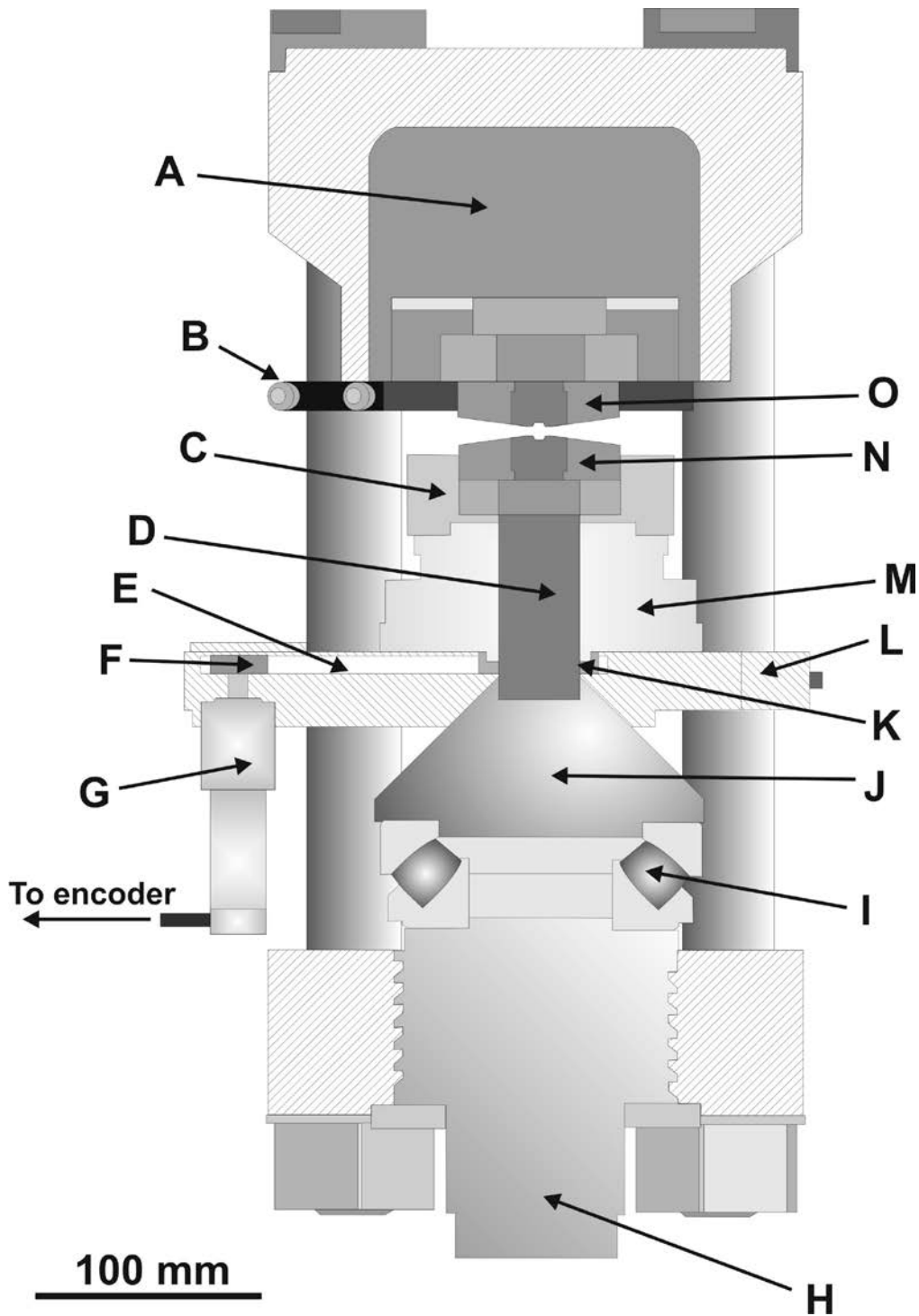


Figure 1 . Cross section of rotating Paris-Edinburgh cell (roPEC) apparatus, based on a modified V7 450 tonne press frame. (A) hydraulic ram, (B) plate preventing rotation of upper (stationary) anvil. This plate is bolted to two of the tie rods, (C) housing for the lower (rotating) anvil, (D) central piston, (E) 3:1 steel-reinforced timing belt, (F) gear-head on externally-mounted servo, (G) externally mounted servo with Harmonic Drive© 100:1 reduction gearing on output, and lined to digital encoder, (H) breech with artillery thread, (I) spherical roller thrust bearings, (J) conical spacer, (K) input gear for reduction gearing, (L) support plate for servo and housing to reduction gearing, (M) 161:1 Harmonic Drive© reduction gearing, (N) lower (rotating) carbide anvil, (O) upper (stationary) carbide anvil.

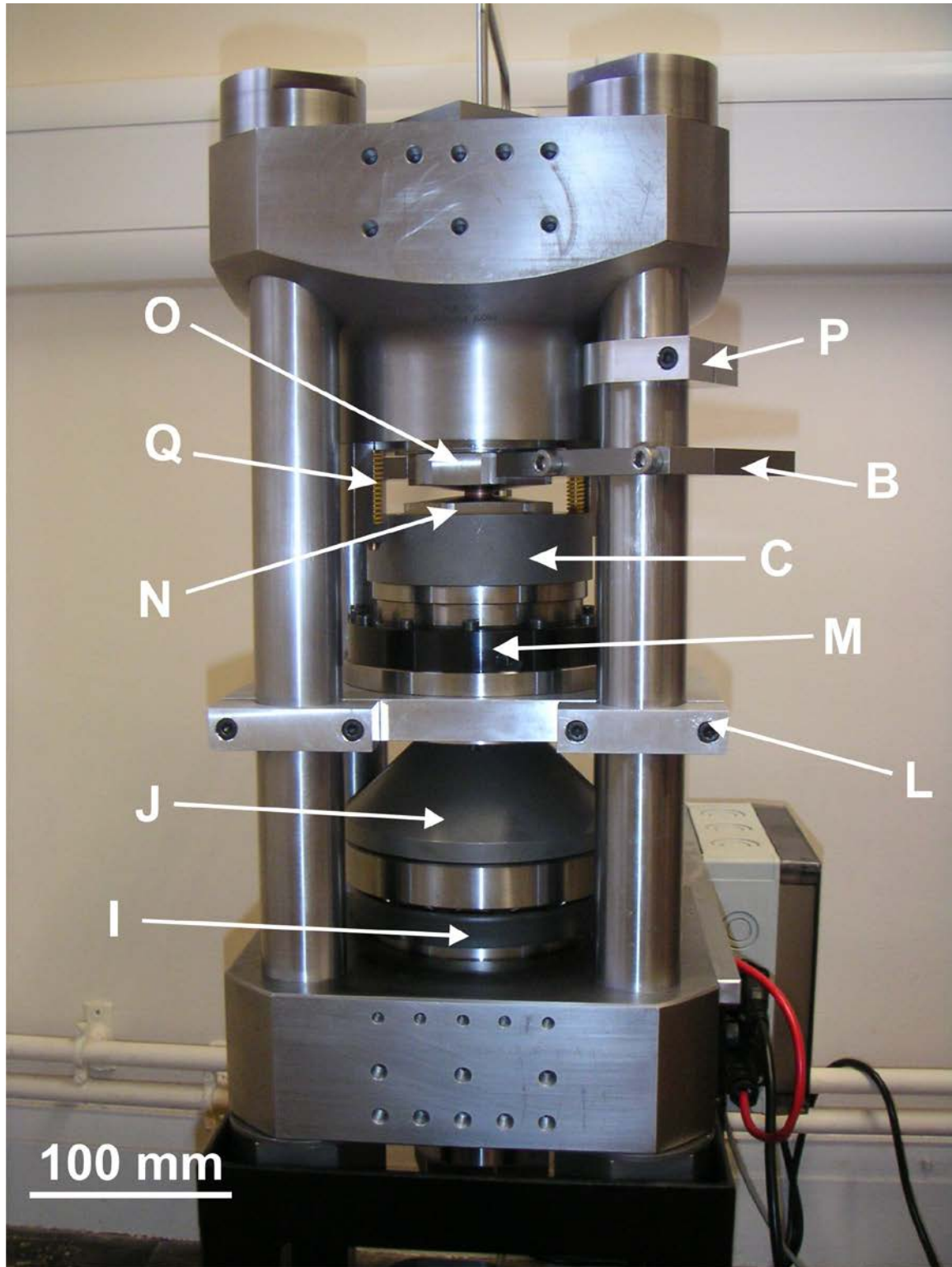


Figure 2. Picture of roPEC. Key as for Figure 1, and (P) bracket used to prevent movement of upper plate due to inversion of press frame (identical bracket on opposing tie-rod), (Q) pair of opposing high tension return springs to facilitate ram head return. Apparatus sits of a small stand to enable access to breech on the underside.

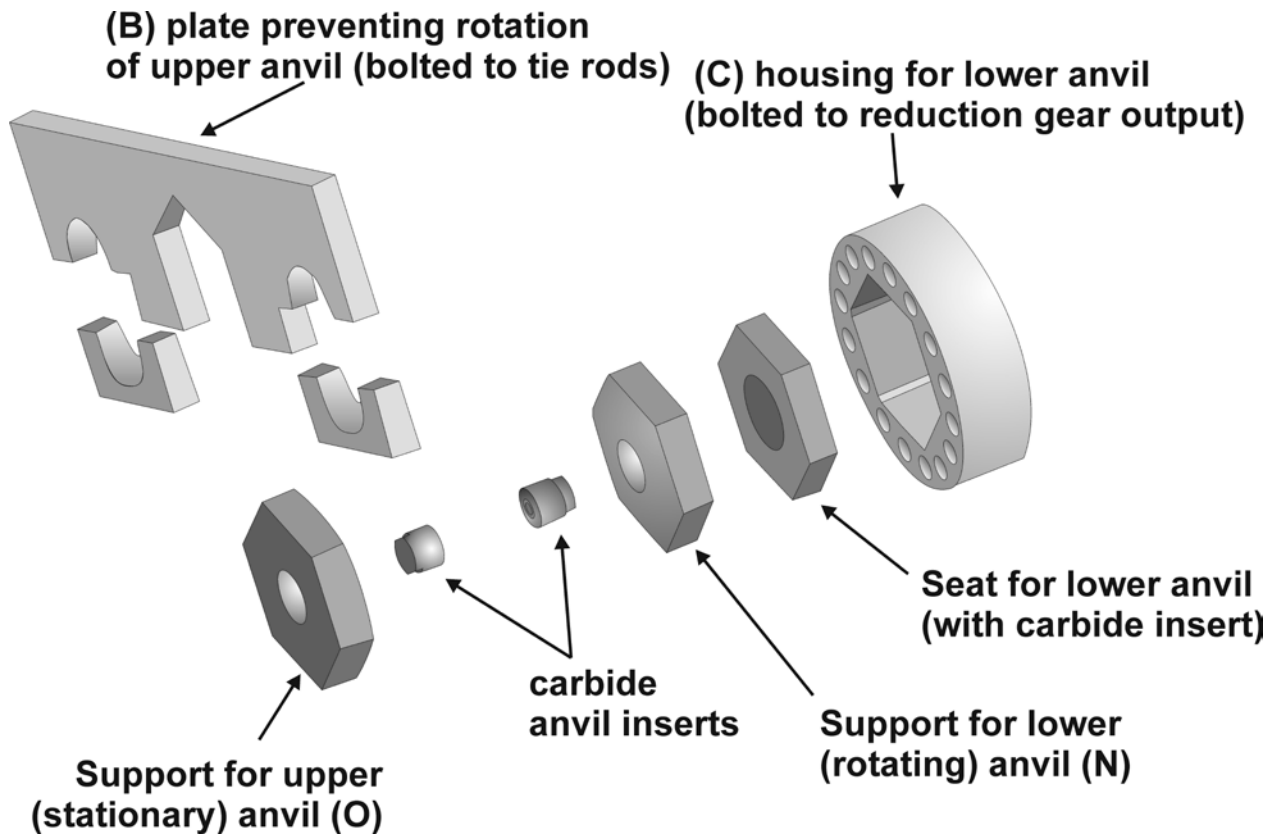


Figure 3. Schematic showing exploded view of anvils and components used to rotate lower anvil and ensure upper anvil remains stationary. Capital letters refer to key used in Figures 1-2.

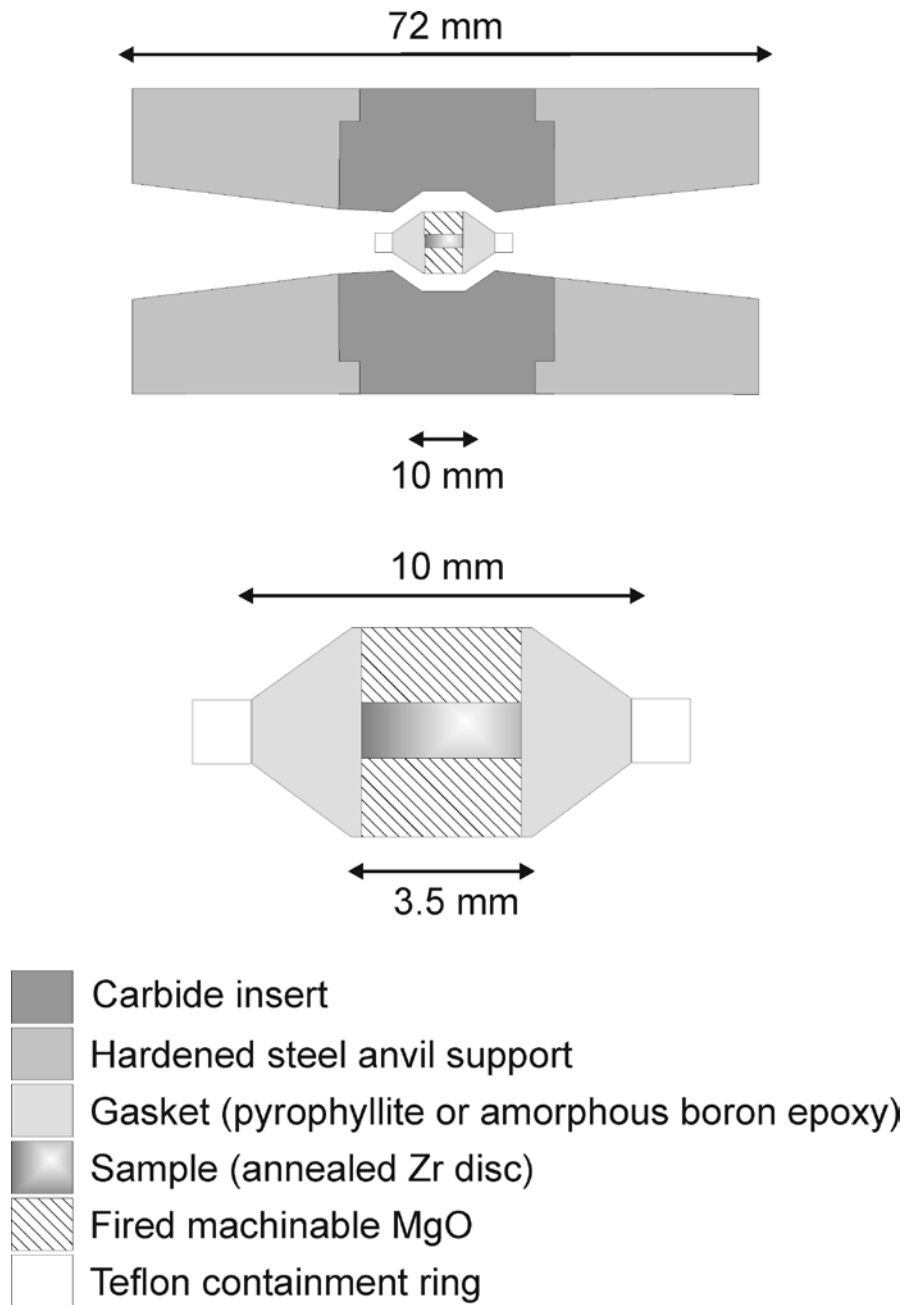


Figure 4. Schematic diagram showing anvil (top) and assembly (bottom) design used in roPEC apparatus.

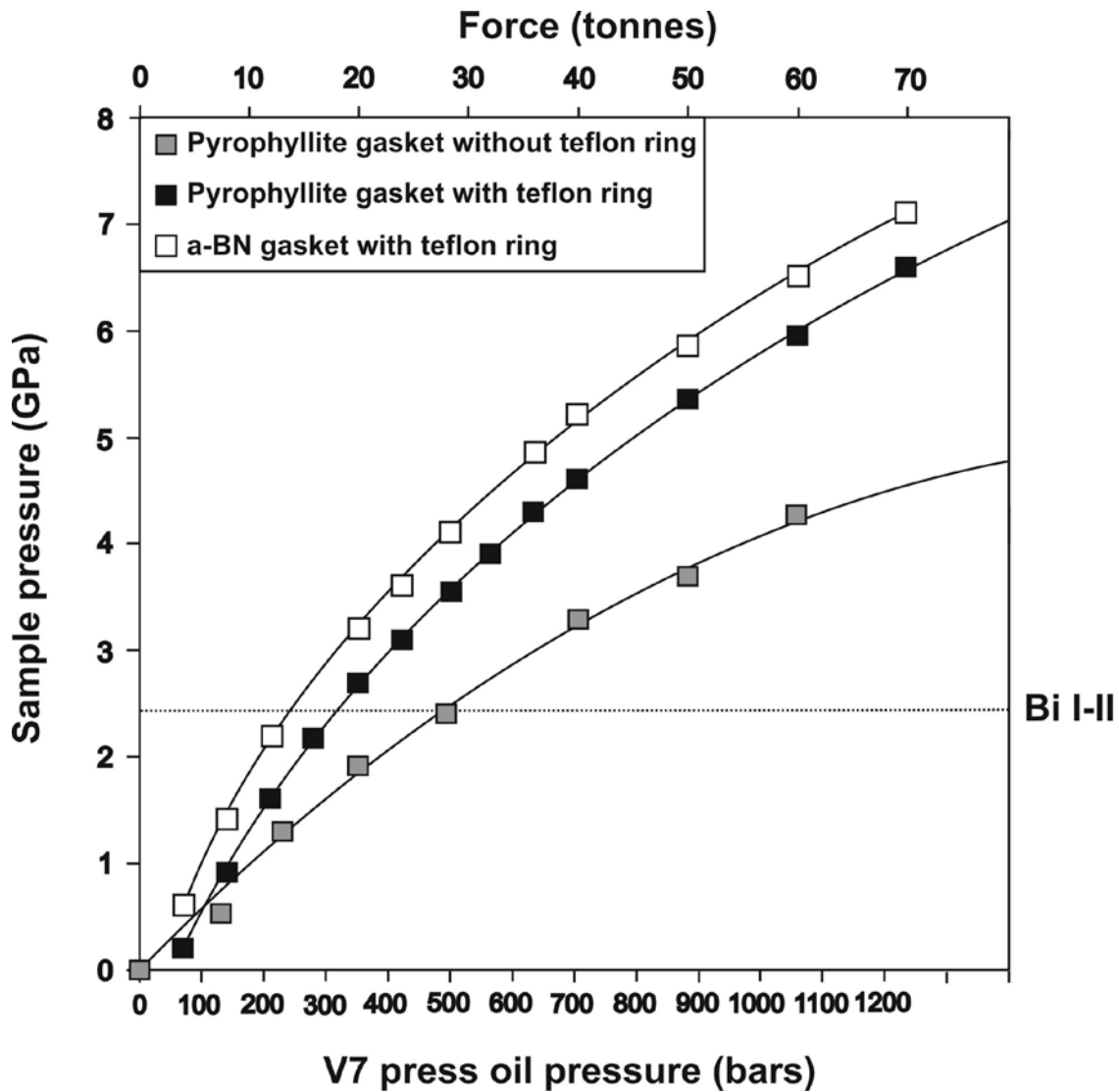


Figure 5. Pressure calibration for pyrophyllite and amorphous-boron epoxy gaskets as described in Figure 4. Calibration curves were determined from several series of *in-situ* X-ray diffraction studies using internal NaCl and MgO pressure standards (using the same gasket/anvil geometry employed for roPEC studies described here). The upper scale indicates force generated by the ram, considering the cross section of the ram is 176.9 cm^2 . Bismuth transition calibration experiments were performed on the roPEC apparatus for a-B epoxy and pyrophyllite gaskets (with Teflon rings). Calibration curve for pyrophyllite gaskets without Teflon ring are shown for comparison.

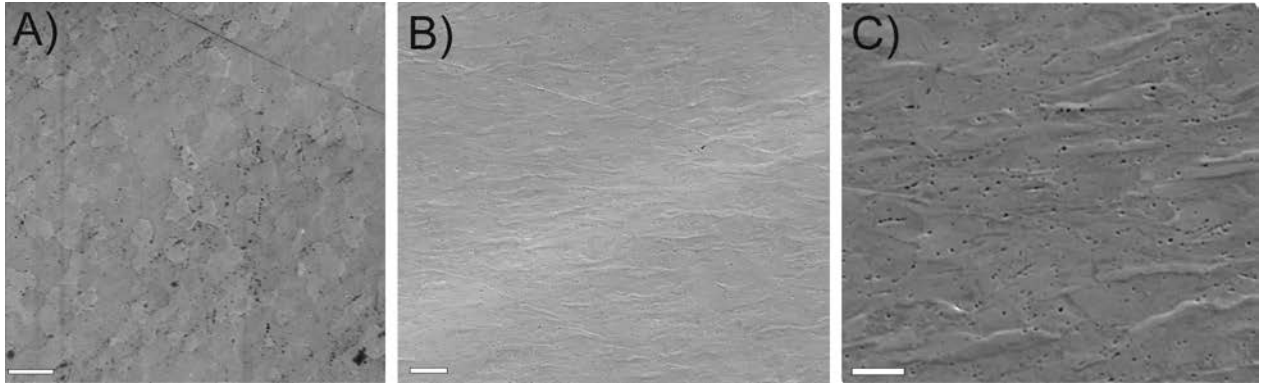


Figure 6. Secondary electron (SEM) images of annealed, polished and etched polycrystalline Zr samples. A) annealed sample compressed to 1.8 GPa but not deformed. B) and C) sample compressed to 1.8 GPa and sheared to strain exceeding $\gamma = 0.9$. In all images white scale bar corresponds to 20 microns. Dark pits and discontinuous dark lines in images A) and C) were formed during surface etching with acid. Other faint straight lines are scratches formed during polishing. In all images direction of compression of the sample is vertical and direction of shear horizontal with respect to the page.

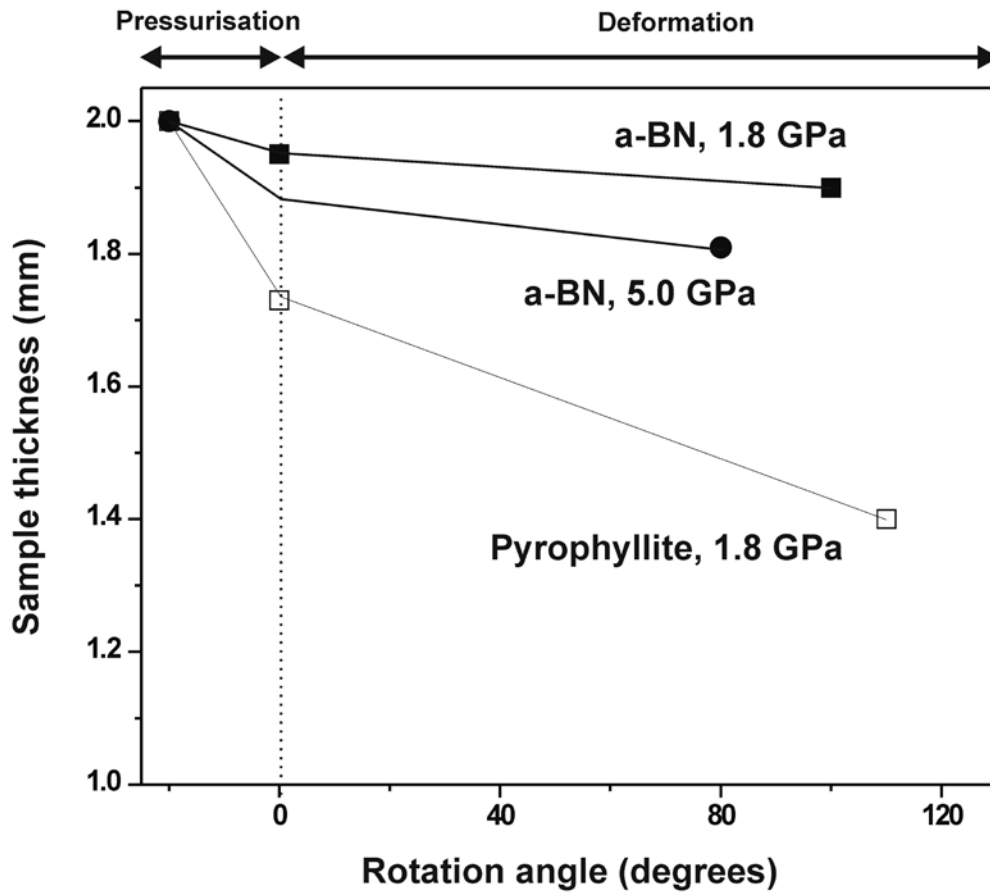


Figure 7. Plot of change in thickness of Zr sample during initial sample pressurisation and following sample deformation in roPEC under different experiment conditions. Sample thickness following pressurisation at 5 GPa was not determined but estimated from changes in ram movement and by comparison with other runs. All runs were deformed at a sample rotation rate of 1.035×10^{-3} rpm.

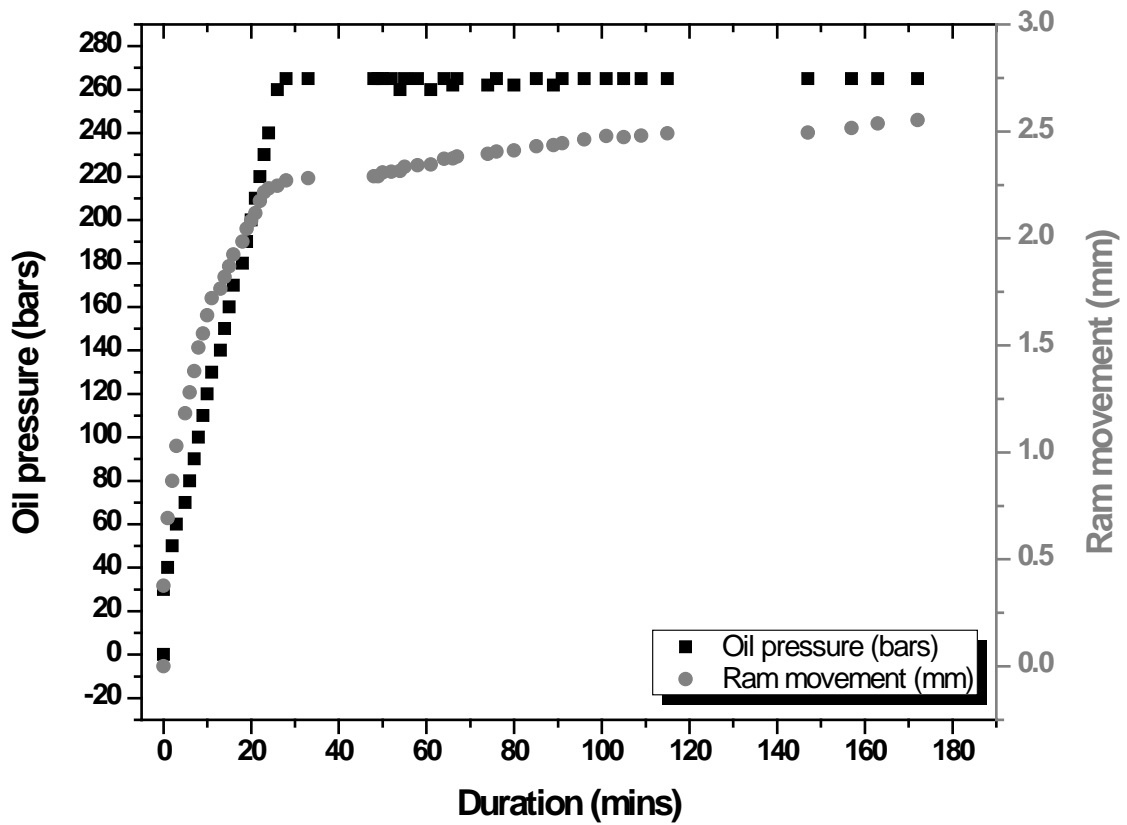


Figure 8. Plot of oil pressure (black squares) and ram movement (grey circles) as a function of experiment duration for experiment performed at 2.5 GPa using an a-B epoxy gasket. Most ram movement occurs during initial pressurisation (first 25 minutes), with minimal additional ram movement once experiment is fully pressurised (25 to 60 minutes). Deformation of the sample commenced at 61 minutes into the experiment, resulting in further ram movement indicative of renewed (minor) gasket flow during sample shear.

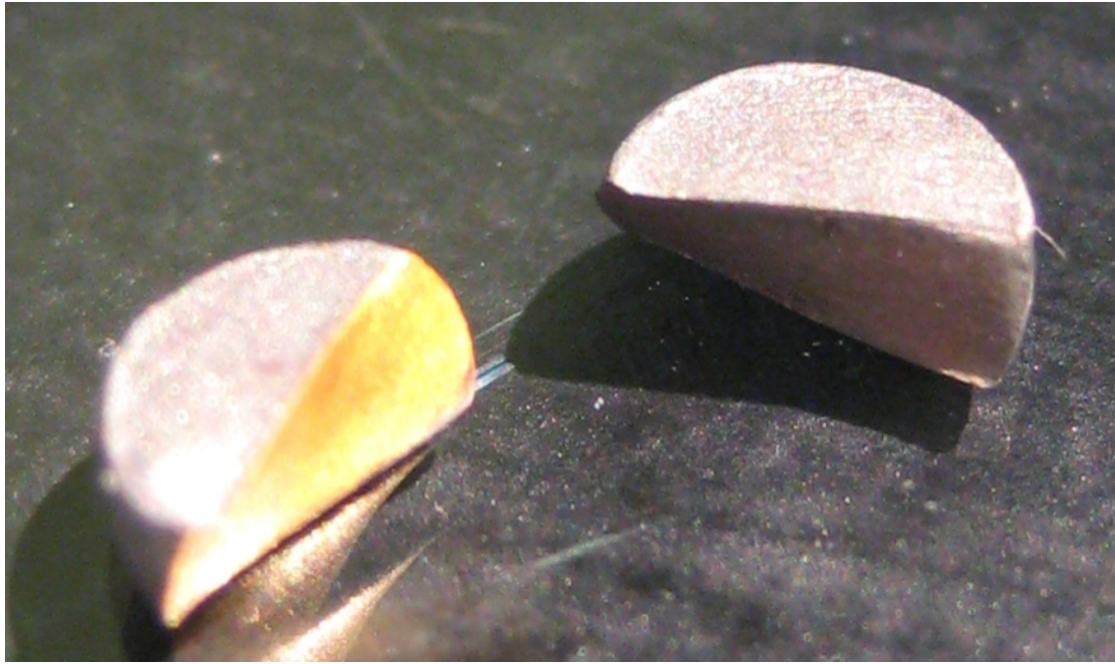


Figure 9. Photograph showing deformed Zr sample (1.8 GPa, pyrophyllite gasket) with internal Au strain marker adfixed (left) to one half of the sample. Sample disc is approximately 1.7 mm thick. At low pressures (below 2-2.5 GPa) and low degrees of total strain, deformed Zr samples could be gently prised apart to show the geometry of the internal strain marker. At high pressures/total strain geometry of the strain marker was determined by observing intersection of Au foil with the sample surface and by sectioning the sample using a wire saw [4].

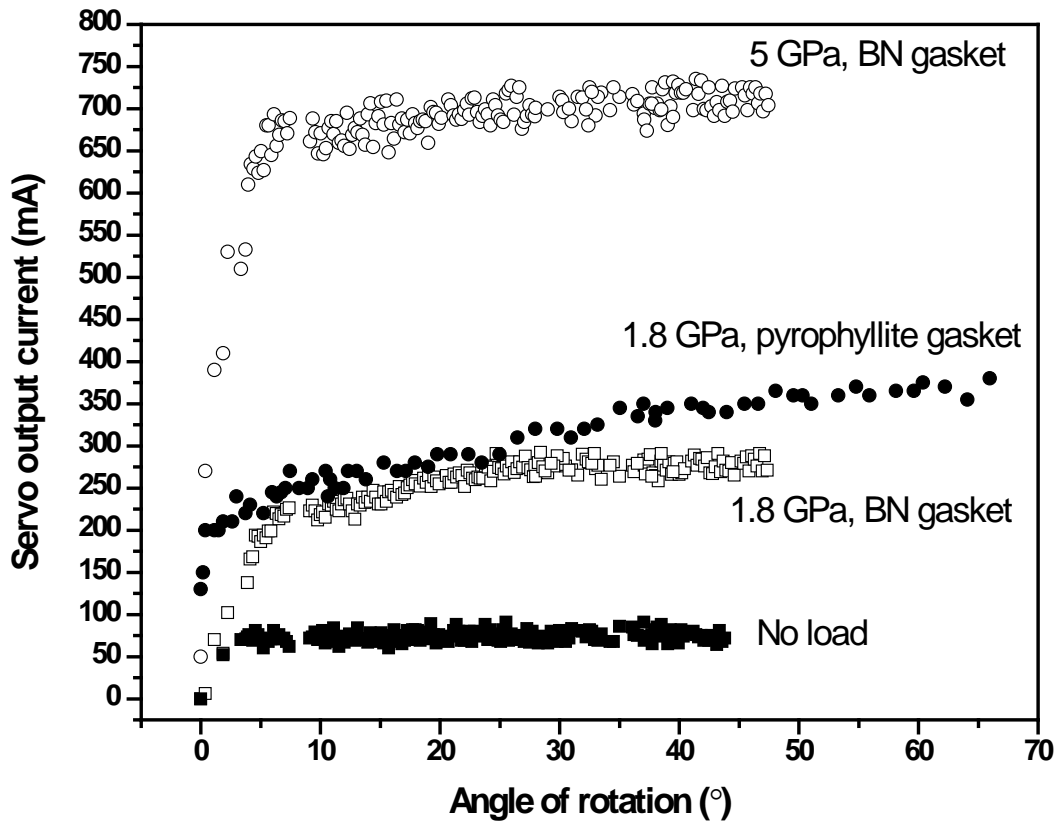


Figure 10. Plot of servo output current (which gives a measure of torque applied by the reduction gearing onto the sample assembly) during prolonged sample deformation under various conditions. All experiments were conducted using a rotation rate of 50 rpm at the servo head, corresponding to a sample rotation rate of 1.035×10^{-3} rpm or approximately $22.3^\circ/\text{hour}$. The ‘no load’ experiment was performed by rotating the apparatus without loading a sample assembly or applying any axial load.

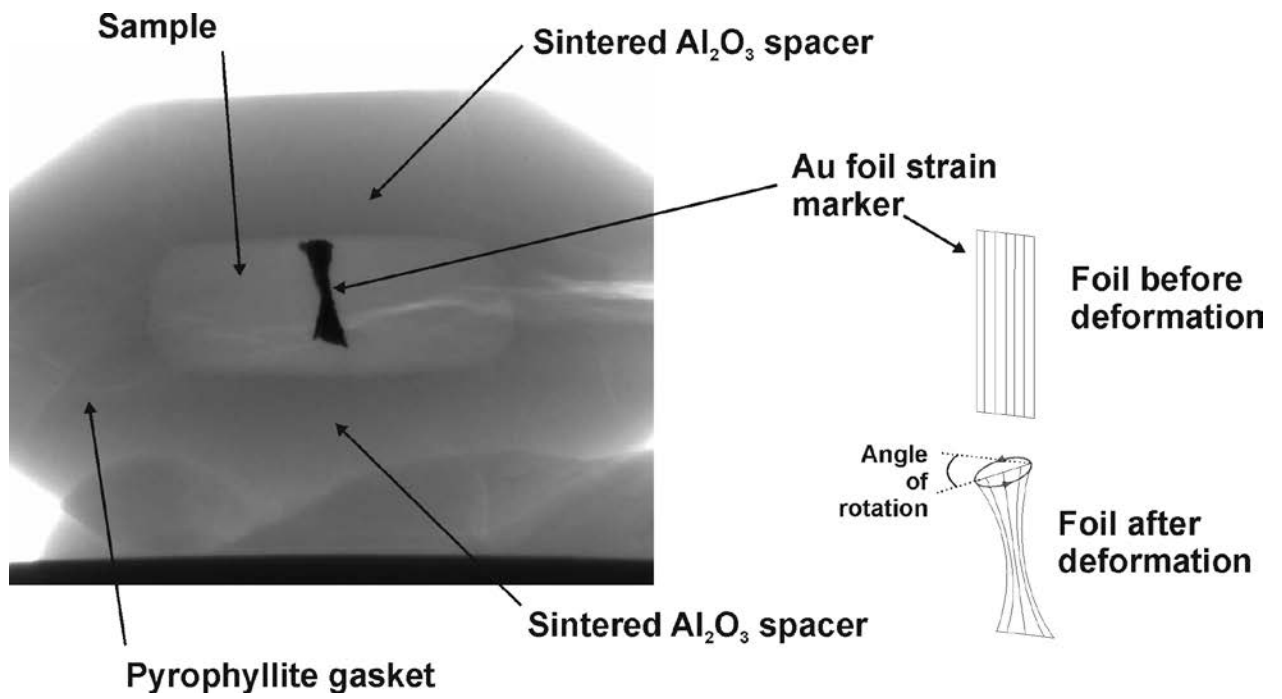


Figure 11. X-ray tomographic image of recovered roPEC sample. Sample (pressed graphite pellet with internal Au foil strain marker) was loaded into a fired pyrophyllite gasket assembly as shown in Figure 4, and deformed at 1 GPa.